IJEIM: Innovative Application Research and Education (ICIARE2013) Vol.4, No.1, 2014

Development and Verification of Multi-Sensing Device attached PZT Patches for Structural Health Monitoring

Tetsuya Morisaki*, Issei Uchitomi, Yuki Higashinaka
Department of Mechanical & Electrical Engineering. Tokuyama Collage of Technology, Japan

Abstract: Structural Health Monitoring (SHM) technique is generally classified into Global and Local SHM techniques. The purpose of the Local SHM technique is to detect initial deteriorations somewhere in a large structure. However, it often requires a sensor network consisting of a large number of sensor devices and they should be small so they can be attached to anywhere. Considering such backgrounds, we constructed a compact, inexpensive and on-site sensor device using PZT patches for the Local SHM. The sensor device has two analog processing circuits for implementing Multi-Sensing. Using the circuits, the sensor device obtains waveform-data for Electrical Impedance and Pulse-Echo analyzing methods for the Local SHM. In addition, wireless communication among the sensor devices and a data log server is provided for accumulating and analyzing. In experiments for verifying a trial production, we presented an effective signal processing methods for detecting quantitative damage represented as a progressing modeled crack and decreasing/increasing tensile force.

Key-Words: *Structural Health Monitoring, Electrical Impedance, Pulse-Echo, Piezocell Patch*

1. Introduction

Structural Health Monitoring (SHM) technique is generally classified into Global and Local SHM techniques. Because the most important aiming of the Global SHM technique is to macroscopically monitor behaviors of a structure, it is easy to diagnose whether the structure has kept or lost significant functions. This means not to detect initial deteriorations in the structure before they progress to a serious state. Conversely, the purpose of the Local SHM technique is to detect such initial deteriorations somewhere in a large structure. However, it often requires a sensor network consisting of a large number of sensor devices that should be small for attaching anywhere.

Considering such backgrounds, we constructed a compact, inexpensive and on-site sensor device for the Local SHM using piezocell (PZT) patches. The PZT patch provides good performance as a sensing and actuating material for Impedance analyzing methods [1-2], Pulse-Echo analyzing methods [3-4], which are promising approaches in the field of Local SHM. Moreover, the PZT patch is easy to install on structure because it is generally bonded to a surface of a specimen using an adhesive.

In order to bring out the abilities of the PZT patch, we present a sensor device, which has a microprocessor with an Analog-to-Digital Converter (ADC), a switching circuit and two analog processing circuits for implementing multi-sensing. In addition, wireless communication among the sensor devices and data log server is provided for real-time structural damage assessments. In experiments for verifying a trial production, we presented an effective signal processing methods for the obtained results of the system to detect quantitative damage represented as a progressing modeled crack and decreasing/increasing tensile force.

2. Constructed System

Received: 20, 11, 2013, Accepted: 03, 12, 2013
*Corresponding author: Tetsuya Morisaki
Email: morisaki@tokuyama.ac.jp

The type of waves generated on a structure by the PZT patch is classified into standing and travelling waves. The techniques are based on an active sensing for the Local SHM. In Impedance Measuring analysis, the standing-wave is swept through a frequency range and the response is analyzed in the frequency domain. The travelling wave is used with time domain analysis, which is represented by Pulse-Echo analysis. To apply the proposing sensor device in this study to both of the analysis methods, we designed two analog processor circuits and assembled the trial production using an ADC (10[bit], 907473[sps], 512[pt]) in a microprocessor (MPU), a switching circuit and Xbee wireless module shown in Fig. 1. The analog processors are respectively consisted of a transmitter and a receiver with the switching circuit.

Figure 2 shows a steel element beam under axial tensile force *P* for evaluating the sensor device. Three PZT patches(C-6 t=0.3[mm]) were bonded at both sides of the beam with a conductive epoxy resin-based adhesive. The crack model was introduced after the inspection of an influence of *P*.

3. Electrical Impedance Analysis

Electrical impedance of the PZT patches is related to a generated standing wave. To generate the wave, a continuous sinusoidal signal (1.0[Vpp]) in a frequency *f* directed by the MPU is outputted from the transmitter in the Analog Processing Circuit for Impedance Analysis. Since the wave is related to various mechanical conditions of the beam, we can detect the changing of the condition with continuously monitoring the electrical impedance. To measure the electrical impedance, reference resistance *Z* is connected to the PZT patches in serial by a receiver in the circuit. For more specialized monitoring the boundary condition, PZT1 and PZT2 are connected to the transmitter in parallel because a longitudinal wave is generated in the direction along the length of the beam by vibrating PZT1 and PZT2 in the same phase. Consequently, the measurement circuit is consistent as shown Fig.3.

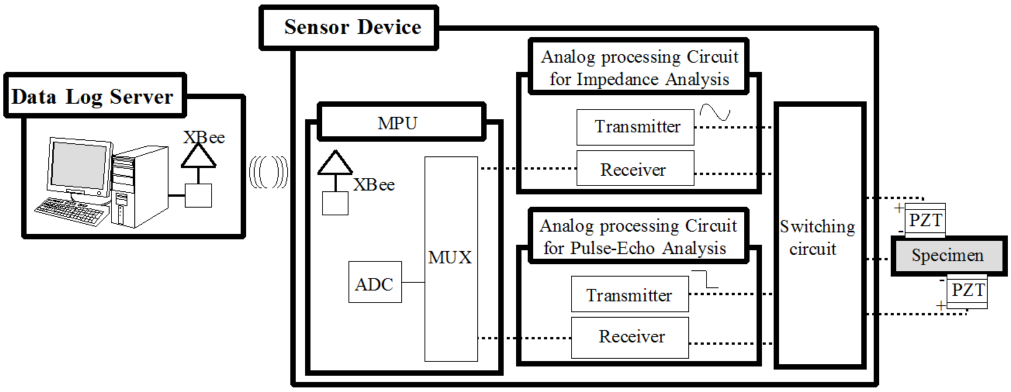

Fig. 1 Outline of the proposing sensor device and monitoring system

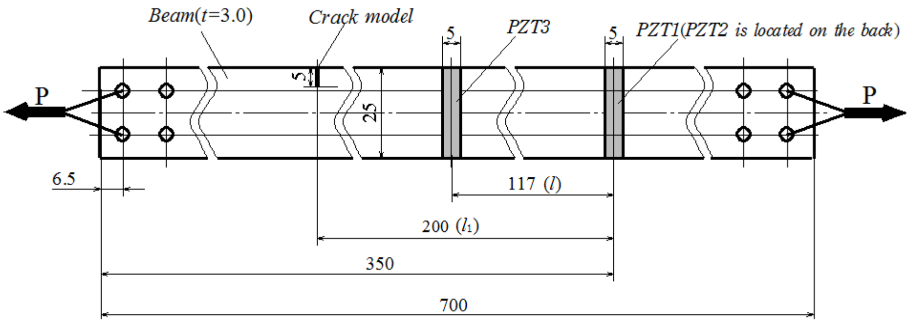

Fig. 2 The steel element beam embedded with PZT patches under axial tensile force *P* and a crack model introduced after the inspection of an influence of *P*

In this way, real part of the electrical impedance $Re(\mathbf{Z}_P)$ of the pair of PZT patches can be obtained as follows. An outputting signal from the receiver to the MPU is successively selected among $\mathbf{V}_F(=\mathbf{V}_F\text{-GND})$, $\mathbf{V}_Z(=\mathbf{V}_F\text{-}\mathbf{V}_Z)$ and $\mathbf{V}_P(=\mathbf{V}_Z\text{-GND})$ using a differential amplifier. The MPU calculates the most probable values of $|\mathbf{V}_F|^2$, $|\mathbf{V}_Z|^2$ and $|\mathbf{V}_P|^2$ from AD converted waveform-data of $\mathbf{V}_F$, $\mathbf{V}_Z$ and $\mathbf{V}_P$ using least-square method with directed frequency f. The procedure is repeated 50 times for averaging and then $|\mathbf{V}_F|^2$, $|\mathbf{V}_Z|^2$ and $|\mathbf{V}_P|^2$ are sent to the data log server using wireless communication. Finally, $Re(\mathbf{Z}_P)$ is calculated by

$$Re(\mathbf{Z}_P)=\frac{|\mathbf{V}_F|^2-|\mathbf{V}_Z|^2-|\mathbf{V}_P|^2}{2|\mathbf{V}_Z|^2}Z \qquad (1)$$

By sweeping the frequency f during interest range, we then obtain $Re(\mathbf{Z}_P)$ in the frequency domain. Figure 4 shows the experimental results of giving tensile axial force P, 10[kgf]. Many peaks are clearly recognized during the measured range. Since the peak frequency relates to resonance frequency of the vibration mode of the beam element, changed tensile axial force of the beam can be detected with monitoring the peak of $Re(\mathbf{Z}_P)$. To verify the performance, we set the P to 20 [kgf] and measured $Re(\mathbf{Z}_P)$.in detail for the peaks shown in Fig. 4. Moreover, the experiment was repeated to check the dispersion. For example, the results around the peak marked with an arrow in Fig. 4 are shown in Fig. 5. Through the experiments, we confirmed that impedance peaks measured by the proposing system shift to higher frequency with changing tensile axial force in enough accuracy for the Local SHM.

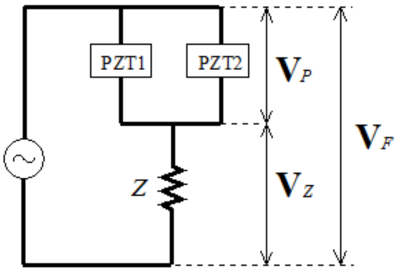

Fig. 3 The diagram of the electrical impedance measurement circuit

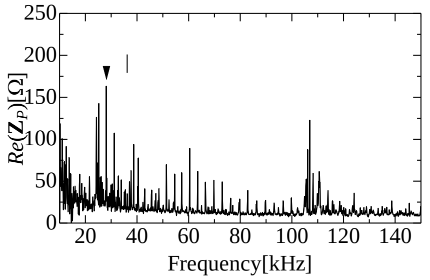

Fig. 4 The experimental result of measuring $Re(\mathbf{Z}_P)$ with tensile axial force P

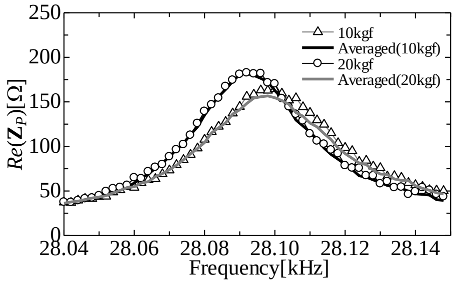

Fig. 5 The 5 times repeated Impedance monitoring results with variation of tensile axial force P

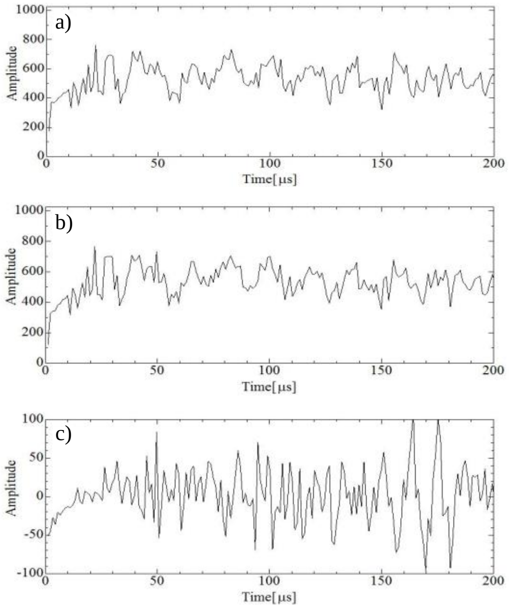

Fig. 6 The waveforms obtained a) before and b) after introducing the crack model and c)the difference between a) and b)

4. Pulse-Echo Analysis

In this section, we describe experiments with the crack model. Then, PZT1 and PZT3 are respectively connected to the transmitter and the receiver in the Analog Processing Circuit for Pulse-Echo Analysis using the switching circuit. The transmitter outputs a step-down signal(24-0[V]) to generate a travelling wave from PZT1. Simultaneously, ADC starts sampling the signal amplified the echo signal of PZT3 via the receiver. The procedure is repeated 50times to reduce noise and obtain waveform-data with sufficiently high accuracy. The averaged result is sent to the data log server using wireless communication.

Figure 6 shows the accumulated waveform-data and the inspecting waveform-data obtained before and after introducing the crack model, as well as the difference of the two. We confirmed that random error is reduced by enough averaging. However, it is difficult to specify factors for echo generation sources because waveform contains a lot of frequency components and it is important to well understand the various properties of wave, especially the relation between frequency and propagating velocity. In order to clear the relation, we applied the waveforms to Wavelet-Transform analysis. The analyzed results obtained from Fig. 6(a) and Fig. 6(c) are shown in Fig.7. The echo signal generated by the crack model clearly appeared at the marked region in Fig. 7(b). The wave propagating velocity c_v in the frequency range of the marked region is 5571[m/s] (=117[mm]/21[μs]) because the echo signal in the frequency range appeared at 21[μs] in Fig. 7(a) and the propagating distance l between PZT1 and PZT3 is 117[mm] as shown in Fig. 2. Assuming that the crack model was given on the left side of the beam, the location of the crack model is estimated as follow.

$$l_1 = \frac{l + c_v t_c}{2} \tag{2}$$

where l_1 is distance to the crack model from PZT1 and t_c is time of the detected echo signal generated by the clack model marked region in Fig. 7(b).Since t_c is 50[[μs] as shown in Fig. 7(b), l_1 is estimated as 198[mm]. As a result of the experiment in this section, we show the performance and effectiveness of a time domain analysis of waveform-data obtained by our proposal.

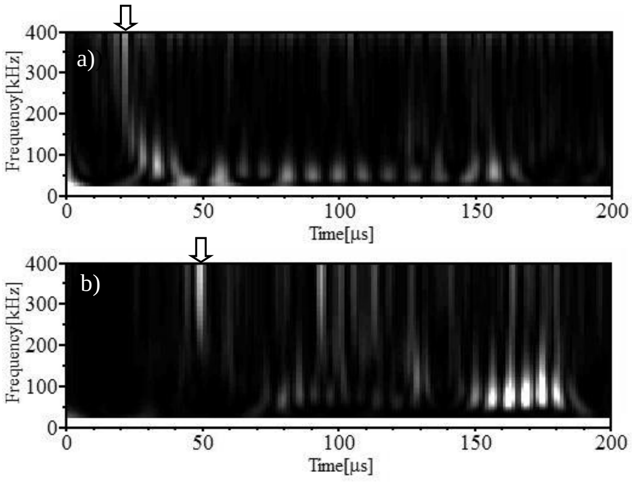

Fig. 7 The Wavelet-Transform results a) and b) obtained from waveform-data shown in Fig. 6(a) and (c) respectively (Image contrast was modified for printing)

5. Conclusion

In this study, we developed a multi-sensing device for the SHM. The device has the ability to monitor a structural condition using standing and travelling waves generated by PZT patches. In the experiments of variation of tensile axial force and crack detection, we confirmed that the accuracy was enough for achieving the Local SHM.

References:

[1] Dansheng Wang and Hongping Zhu, “Monitoring of the strength gain of concrete using embedded PZT impedance transducer” Construction and Building Materials, Volume 25, Issue 9, September 2011, pp 3703–3708

[2] Wieslaw Ostachowicz, Pawel Kudel, Pawel Malinowski and Tomasz Wandowsk, “Damage localization in plate-like structures based on PZT sensors” Mechanical Systems and Signal Processing, 23, 2009, pp1805–1829

[3] Yong Hong, Seung Ho Hwang, Gao Ping Wang and Dong Pyo Hong, “Application Technique of PZT Sensors to Detect Structural Damage”, KEY ENGINEERING MATERIALS; Vol. 385-387, 2008, pp729-732

[4] Liu, Xinglong, Zhou, Chengxu and Jiang, Zhongwei, “Damage localization in plate-like structure using built-in PZT sensor network”, Smart structures and systems, Vol. 9, NO.1,2012 , pp.21-33